Archival Report

Biological Psychiatry: CNNI

Aberrant Hierarchical Prediction Errors Are Associated With Transition to Psychosis: A Computational Single-Trial Analysis of the Mismatch Negativity

Daniel J. Hauke, Colleen E. Charlton, André Schmidt, John D. Griffiths, Scott W. Woods, Judith M. Ford, Vinod H. Srihari, Volker Roth, Andreea O. Diaconescu, and Daniel H. Mathalon

ABSTRACT

BACKGROUND: Mismatch negativity reductions are among the most reliable biomarkers for schizophrenia and have been associated with increased risk for conversion to psychosis in individuals who are at clinical high risk for psychosis (CHR-P). Here, we adopted a computational approach to develop a mechanistic model of mismatch negativity reductions in CHR-P individuals and patients early in the course of schizophrenia.

METHODS: Electroencephalography was recorded in 38 CHR-P individuals (15 converters), 19 patients early in the course of schizophrenia (≤5 years), and 44 healthy control participants during three different auditory oddball mismatch negativity paradigms including 10% duration, frequency, or double deviants, respectively. We modeled sensory learning with the hierarchical Gaussian filter and extracted precision-weighted prediction error trajectories from the model to assess how the expression of hierarchical prediction errors modulated electroencephalography amplitudes over sensor space and time.

RESULTS: Both low-level sensory and high-level volatility precision-weighted prediction errors were altered in CHR-P individuals and patients early in the course of schizophrenia compared with healthy control participants. Moreover, low-level precision-weighted prediction errors were significantly different in CHR-P individuals who later converted to psychosis compared with nonconverters.

CONCLUSIONS: Our results implicate altered processing of hierarchical prediction errors as a computational mechanism in early psychosis consistent with predictive coding accounts of psychosis. This computational model seems to capture pathophysiological mechanisms that are relevant to early psychosis and the risk for future psychosis in CHR-P individuals and may serve as predictive biomarkers and mechanistic targets for the development of novel treatments.

https://doi.org/10.1016/j.bpsc.2023.07.011

Often without our awareness, our brain continuously learns about our environment. The mismatch negativity (MMN) is a neurophysiological index of such implicit learning that is commonly measured with electroencephalography (EEG). It refers to a brain response that is elicited automatically when an auditory stimulus violates a statistical regularity in the recent auditory environment (1), for example when a series of low tones is unexpectedly interrupted by a high tone. Formally, the MMN is a transient negative wave deflection in the event-related potential (ERP) elicited by infrequent deviant stimuli randomly interspersed among frequent standard stimuli that is most easily identified between 100 and 250 ms following stimulus onset in the deviant-standard ERP difference wave (2,3).

MMN amplitude reductions in schizophrenia have been demonstrated repeatedly (4). Interest in MMN amplitude reductions as an early warning sign for impending psychosis has increased recently. MMN reductions are already present in individuals who are at clinical high risk for psychosis (CHR-P), likely reflecting vulnerability for a progression to full psychosis because reductions were found to be more pronounced in CHR-P individuals who later converted to a psychotic disorder (5–9). Despite its clinical potential, the mechanisms that account for MMN reductions in CHR-P individuals remain poorly understood. One of the biggest challenges in early detection and intervention research lies in developing novel medications to delay or even prevent transition to psychosis (10). This challenge has been attributed to a lack of mechanistic models of pathophysiological processes, especially in the CHR-P population (10).

Several computational theories of the MMN have been proposed (11–13). One compelling class of theories is Bayesian accounts of the MMN (11,12,14,15). At their core, they assume that the brain actively predicts its sensory

ISSN: 2451-9022

environment. These predictions are compared with incoming sensory inputs, and the discrepancy between predictions and inputs—prediction errors (PEs)—weighted by the confidence with which predictions are made (i.e., the precision thereof) is used to continuously update the brain's internal model of the world. Importantly, recent theories assume that the brain's internal model is hierarchically structured such that lower levels track local (immediate) and higher levels track global (more slowly changing) statistics of the world (14–19). From a Bayesian perspective, evoked responses during an auditory oddball task reflect precision-weighted PE (pwPE) updates of the brain's internal model of the world (11), and MMN reductions in schizophrenia could reflect a failure to compute hierarchical pwPEs adequately.

Interestingly, PEs may be implemented neurally through AMPA receptor signaling and precisions through NMDA receptor (NMDAR) neuromodulatory system interactions (20–22). Consistent with this hypothesis, the NMDAR antagonist ketamine was found to reduce MMN amplitudes in humans (23–25), and 2 pharmacological studies conducted with healthy control participants (HCs) suggest that EEG signatures of hierarchical pwPEs during oddball tasks are also altered by ketamine (14) and muscarinic, but not dopaminergic, interventions (15). Taken together, these results suggest that hierarchical Bayesian models are promising candidates for understanding why the MMN is reduced in schizophrenia and that these models may even serve as computational assays to probe neuroreceptor function noninvasively (26) to identify subtypes with impairments in specific neuroreceptor systems (15,27–29) or critical time windows for early interventions.

We applied a hierarchical Bayesian modeling approach (14,30,31) to EEG data from a previously published study (8) to develop a mechanistic model of altered information processing as a basis for MMN amplitude reductions in CHR-P individuals and patients with early-illness schizophrenia (ESZ). This study found reduced MMN amplitudes in patients with ESZ and CHR-P individuals and furthermore showed MMN deficits to be greater in those CHR-P individuals who subsequently converted to psychosis compared with nonconverters who were followed for at least 12 months (8). In this study, we investigated what changes in information processing underlie these effects.

METHODS AND MATERIALS

Participants

Participants included 19 patients with ESZ (≤5 years since initial hospitalization or initiation of antipsychotic medication; age [mean ± SD] 19.97 ± 5.50 years, range 13–37 years) (Table 1), 38 CHR-P individuals (age 17.40 ± 3.50 years, range 12–26 years) (Table 1), and 44 HCs (age 23.91 ± 6.17 years, range 12–37 years) (Table 1) (8). CHR-P participants were followed for over 24 months. Fifteen CHR-P individuals converted to full psychosis (CHR-C) (time-to-conversion 10.42 ± 9.01 months); 16 CHR-P individuals did not convert (CHR-NC) but were followed for at least 12 months (follow-up duration 28.59 ± 8.80 months). Seven individuals from the CHR-P group dropped out before the 12-month follow-up and were excluded from analyses comparing CHR-C and CHR-NC groups because their clinical outcomes were uncertain. Recruitment and inclusion and exclusion criteria are detailed in the Supplement and in the original study (8). The study was approved by the Institutional Review Board of Yale University, and all adult participants provided written informed consent. For minors, parents provided written informed consent, and minors provided written assent.

Task

Participants performed an unrelated primary task (silently reading a book) while being presented with three auditory oddball paradigms presented in a fixed order (Figure S1). Each paradigm comprised two runs of 875 tones each (1750 tones in total), including 90% standard tones (50 ms, 633 Hz) and either 10% duration (100 ms), 10% frequency (1000 Hz), or 10% duration + frequency double deviants (100 ms and 1000 Hz). All tones were presented at 78 dB in fixed pseudorandomized order with 5-ms rise/fall times and 510-ms stimulus onset asynchrony through Etymotic ER3-A insert earphones (Etymotic Research, Inc.).

EEG Data Processing

EEG was recorded using a 20-channel electrode cap with a standard 10–20 montage (Physiometrix, Inc.) and additional mastoid and nose electrodes with linked-ear reference and an FPz ground. Signals were digitized at 1000 Hz with a Neuroscan Synamps amplifier (NeuroscanA). Electro-oculograms were recorded from electrodes located above and below the left eye and at the outer canthi of both eyes.

EEG preprocessing consisted of high-pass filtering with a Butterworth filter (0.5 Hz), downsampling (256 Hz), and low-pass filtering using a Butterworth filter (30 Hz), followed by epoching into 500-ms segments around tone onsets (−100 to 400 ms), baseline correction (−100 to 0 ms), and eyeblink correction using principal component analysis with one component (Supplement). Subsequently, remaining artifactual trials were rejected using a ±100-μV amplitude threshold. Preprocessing and statistical analyses were implemented in MATLAB (version 2020b; The MathWorks, Inc.; https://mathworks.com) using the SPM12 toolbox (version 7771, https://www.fil.ion.ucl.ac.uk/spm/software/spm12/).

Computational Modeling

We modeled implicit sensory learning about the tone sequences with a 3-level binary hierarchical Gaussian filter (HGF) (30,31); see the Supplement for modeling details. This model assumes that participants make inferences about hidden states of the environment (Figure 1A). In the oddball paradigm, participants need to learn about a low-level hidden state $x_2^{(k)}$, which represents the tendency of a specific tone to be prevalent in the environment (tone tendency) and whether the environment is stable or changing (i.e., volatile) captured by the high-level state $x_3^{(k)}$ based on each trial input (standard or deviant tones). We chose a 3-level over a 2-level HGF because we assumed that participants' brains implicitly track local changes in deviant probability that occur throughout the task

Table 1. Demographic and Clinical Characteristics of Study Participants

Characteristic	HC, n = 44	CHR-P, n = 38	ESZ, n = 19	Test Statistic	Post Hoc Contrasts	CHR-C, n = 15	CHR-NC, n = 16	Test Statistic
Age, Years	19.97 (5.50)	17.40 (3.50)	23.91 (6.17)	$F_{2,98} = 10.838$, $p < .001$	ESZ > HC ESZ > CHR-P	17.47 (2.18)	15.88 (3.27)	$F_{1,29} = 2.475$, $p = .127$
Sex, Female/Male	17/27	15/23	4/15	$\chi^2_2 = 2.178$, $p = .337$		6/9	7/9	$\chi^2_1 = 0.045$, $p = .833$
Handedness[a], Right/Left/ Ambidextrous	37/5/2	31/3/4	16/1/2	$\chi^2_4 = 1.765$, $p = .779$		13/1/1	12/1/3	$\chi^2_2 = 1.009$, $p = .604$
Socioeconomic Status[b]	28.02 (13.17)	36.64 (15.22)	40.44 (9.06)	$F_{2,96} = 6.959$, $p = .002$	ESZ > HC ESZ > CHR-P	36.70 (13.39)	35.34 (18.01)	$F_{1,29} = 0.056$, $p = .815$
Race/Ethnicity				$\chi^2_8 = 23.937$, $p = .002$	ESZ ≠ HC CHR-P ≠ HC			$\chi^2_3 = 2.031$, $p = .556$
African American	2	5	8			2	1	
American Indian	0	0	0			0	0	
Asian	4	1	0			0	0	
Caucasian	37	26	9			9	13	
Hispanic	1	4	2			3	1	
Pacific Islander	0	0	0			0	0	
Other	0	2	0			1	1	
High Risk Type[c]								$\chi^2_2 = 2.004$, $p = .367$
APS		38				15	16	
BLIP		1				1	0	
GRD		1				1	0	
Diagnostic Type								
Catatonic			1					
Disorganized			1					
Paranoid			11					
Residual			1					
Schizoaffective			3					
Undifferentiated			2					
Antipsychotic Type				$\chi^2_3 = 19.811$, $p < .001$				$\chi^2_1 = 0.860$, $p = .354$
Atypical only		10	13			5	3	
Atypical and typical		1	3			0	0	
Typical only		0	0			0	0	
None		27	2			10	13	
Unknown		0	1			0	0	
PANSS Positive (41)			18.71 (5.78)					
PANSS Negative (41)			17.14 (6.11)					
SOPS Positive (39,40)		11.03 (4.96)				12.47 (5.07)	9.00 (4.91)	$F_{1,29} = 3.739$, $p = .063$
SOPS Negative (39,40)		10.74 (6.35)				14.40 (5.05)	6.69 (5.71)	$F_{1,29} = 15.767$, $p < .001$

Values are mean (SD) or *n*, unless otherwise indicated. All *p* values are uncorrected.

APS, attenuated psychotic symptoms; BLIP, brief and limited intermittent psychotic symptoms; CHR-C, individuals at clinical high risk for psychosis who later converted to a psychotic disorder; CHR-NC, individuals at clinical high risk for psychosis who did not convert; CHR-P, individuals at clinical high risk for psychosis; ESZ, patients with early-illness schizophrenia (≤5 years since initial hospitalization or initiation of antipsychotic medication); GRD, genetic risk and deterioration syndrome; HC, healthy control; PANSS, Positive and Negative Syndrome Scale; SOPS, Scale of Prodromal Symptoms.

[a]Crovitz-Zener questionnaire (62) for handedness.

[b]Parental socioeconomic status as measured with the Hollingshead Four-Factor Index (37) based on maternal and paternal education and maternal and paternal occupational status. Reported are averages across primary and secondary caregiver. Lower values indicate higher socioeconomic status.

[c]High-risk types are not mutually exclusive.

(Figure 1B). Importantly, because the constant global deviant probability is unknown to participants, local changes in deviant probability are ambiguous and could either signal that the environment is about to change or be explained away as noise. Based on previous literature suggesting that the repetition positivity increases with repeated presentation of standard tones (32), we have reason to believe that the brain tracks local changes even in globally stable environments because participants need to continuously infer the appropriate amount of volatility.

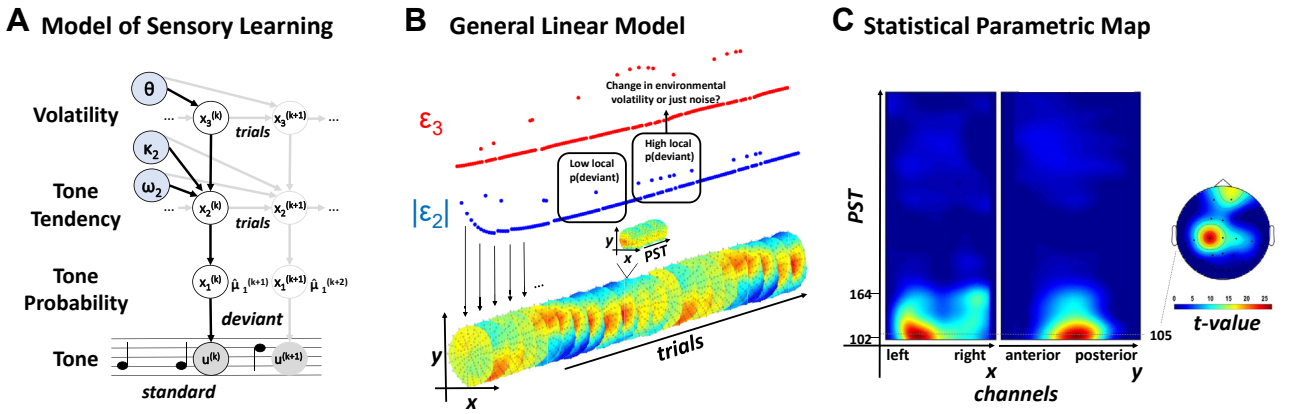

Figure 1. Computational analysis pipeline. **(A)** Trial-by trial trajectories of low- and high-level precision-weighted prediction errors were computed using the hierarchical Gaussian filter (30,31). **(B)** In a first-level analysis, precision-weighted prediction errors were used as parametric regressors to explain electroencephalography (EEG) amplitude variations at each point in sensor space and peristimulus time (PST) following the tone presentation across trials within each participant. Note that the constant global deviant probability is unknown to the participants; thus, periods of high local deviant probability are ambiguous and could either signal an impending change in the environment or just noise. The model assumes that participants need to continuously infer the appropriate amount of volatility of the environment. **(C)** First-level statistics were carried to the second level to obtain statistical parametric maps over 2-dimensional sensor space and peristimulus time.

Participants' beliefs about the hidden states at level *i* of the hierarchy and on trial *k* are denoted with $\mu_i^{(k)}$ and were updated after each new tone according to the following belief update equation:

$$\underbrace{\Delta\mu_i^{(k)}}_{\text{belief update}} \propto \overbrace{\frac{\hat{\pi}_{i-1}^{(k)}}{\pi_i^{(k)}}}^{\text{precision-weight}} \underbrace{\delta_{i-1}^{(k)}}_{\text{prediction error}} \tag{1}$$

where $\mu_i^{(k)}$ is the expectation or belief at trial *k* and level *i* of the hierarchy, $\hat{\pi}_{i-1}^{(k)}$ is the precision (inverse of the variance) from the level below (the hat symbol denotes that this precision has not been updated yet and is associated with the prediction before hearing a new tone), $\pi_i^{(k)}$ is the updated precision at the current level, and $\delta_{i-1}^{(k)}$ is a PE expressing the discrepancy between the expected and the experienced outcome. Because we coded deviant tones as 1 and standard tones as 0, positive low-level pwPEs signal that deviant tones are more frequent than expected, whereas negative low-level pwPEs indicate that standard tones are more frequent than expected (although note that the sign depends on how the input is coded). Conversely, positive and negative high-level pwPEs signal that the environment is more volatile or more stable than expected, respectively. The magnitude of pwPEs is proportional to the belief update, i.e., the extent to which participants need to adjust their internal model of the world after experiencing a new tone.

Consistent with a previous study examining the effects of ketamine on sensory learning in a roving paradigm (14), we focused our analysis on low-level pwPEs about the tone tendency (ϵ_2) and high-level pwPEs about the volatility of the environment (ϵ_3), where the pwPE $\epsilon_i^{(k)}$ on each trial *k* and at level *i* of the hierarchy is defined as (cf. equation 1):

$$\epsilon_i^{(k)} := \frac{\hat{\pi}_{i-1}^{(k)}}{\pi_i^{(k)}} \delta_{i-1}^{(k)} \tag{2}$$

We optimized the parameters of the perceptual model assuming that each participant acted as an ideal Bayesian observer minimizing surprise about input sequences (Table 2). Preferably, model parameters should be estimated based on both input and participants' behavioral responses to quantify how participants' learning deviates from an ideal Bayesian observer. However, this was not possible because the MMN paradigm does not require participants to make responses.

Table 2. Summary of Input and Posterior Parameter Estimates

Variable	HC, *n* = 44	CHR-P, *n* = 38	ESZ, *n* = 19	Statistic	CHR-C, *n* = 15	CHR-NC, *n* = 16	Statistic
Input Entropy	0.47 (0.00)	0.47 (0.00)	0.47 (0.00)	$F_{2,98}$ = 0.522, p = .595	0.47 (0.00)	0.47 (0.00)	$F_{1,29}$ = 0.417, p = .523
Evolution Rate, ω_2	−0.20 (0.78)	−0.19 (0.77)	−0.36 (0.85)	$F_{2,98}$ = 1.862, p = .161	−0.16 (0.82)	−0.22 (0.78)	$F_{1,29}$ = 0.156, p = .696
Metavolatility, ω_3	4.80 (0.30)	4.86 (0.29)	4.80 (0.31)	$F_{2,98}$ = 3.034, p = .053	4.76 (0.29)	4.83 (0.31)	$F_{1,29}$ = 2.651, p = .114

Values are mean (SD) unless otherwise indicated.

CHR-C, individuals at clinical high risk for psychosis who later converted to a psychotic disorder; CHR-NC, individuals at clinical high risk for psychosis who did not convert; CHR-P, individuals at clinical high risk for psychosis; ESZ, patients with early-illness schizophrenia (≤5 years since initial hospitalization or initiation of antipsychotic medication); HC, healthy control.

Statistical Analyses

Demographic and clinical variables were analyzed in R (version 4.04; https://www.r-project.org/) using R-Studio (version 1.4.1106; https://www.rstudio.com/). We report uncorrected p values for either analyses of variance or χ^2 tests, as appropriate. Post hoc tests were Bonferroni corrected ($\alpha = 0.05$).

First-Level Analysis. We extracted the trajectories of low-level pwPEs about the tone tendency ϵ_2 and high-level pwPEs about environmental volatility ϵ_3. Trial-by-trial magnitude estimates of the absolute value of low-level pwPEs $|\epsilon_2|$ or high-level pwPEs ϵ_3 were included as parametric regressors to explain trial-by-trial variation in EEG amplitude (Figure 1B) as done previously (14). The absolute value of ϵ_2 was chosen because it expresses Bayesian surprise independent of the physical characteristics of a tone such as a specific frequency.

Note that taking the absolute value also means that the 10% largest $|\epsilon_2|$ are elicited for both deviants (about 67.25% on average across all input sequences) and standards (32.75%). The standard tones also elicit large $|\epsilon_2|$, but only in the beginning of the experiment, because participants do not yet know which tone will be the standard tone. Conversely, the 10% lowest $|\epsilon_2|$ trials correspond exclusively to the standard condition of the classical MMN. The 10% largest and smallest ϵ_3 are elicited by deviant (99.94%) and standard (100%) tones, respectively, because deviant tones could signal that the environment is about to change (i.e., when the local frequency of deviants is $>$ 10%, e.g., 2 deviants in a row). It must be noted that these statistics apply only to the current design and will differ for other tone sequences.

The general linear model at the first level consisted of an intercept term and either (z-standardized) low- or high-level pwPE trajectories as predictors and EEG amplitude across sensors and peristimulus time as the response variable. For each pwPE, we tested the null hypothesis that the parameter estimate was 0 at each sensor and time point using an F test. As an additional test to assess whether high-level pwPEs derived from the third level of the HGF explained additional variance in the EEG, suggesting that the brain tracks changes in local deviant probability despite the globally stable deviant probability, we also conducted a supplementary analysis in which we included both low- and high-level pwPEs in the same first-level general linear model and tested whether high-level pwPEs still explained a significant amount of variance. The results of this analysis suggested that they did (Figure S5). Statistical analyses were restricted to 100- to 400-ms post-stimulus time consistent with previous analyses (14,33) to include the MMN and P300 peaks and to constrain the number of statistical tests.

Second-Level Analysis. First-level statistics were converted into images and smoothed using a Gaussian kernel (full width at half maximum: 16 mm $\times$ 16 mm) to ensure that the assumptions of Gaussian random field theory were met (34,35). Smoothed images were carried to the second level to compare groups using different factorial designs for each pwPE to obtain statistical parametric maps over 2-dimensional sensor space and peristimulus time (Figure 1C and Figure S2). Each factorial design included group as a between-subjects and oddball paradigm as a within-subject factor. When comparing the HC, CHR-P, and ESZ groups, we also included (z-standardized) age as a covariate that was allowed to interact with group (Figure S6) to account for age differences across these groups (Table 1). Multiple testing correction was implemented using Gaussian random field theory (Figure S3) (34,35). We report p values corrected for peak-familywise error rates (p_{pFWE}) or cluster-level FWE rates (p_{cFWE}) using a cluster-defining threshold of $p < .001$ (36) unless stated otherwise.

RESULTS

Group Differences in Low-Level pwPEs

We observed a significant effect of group on the expression of low-level pwPEs about the tone tendency ϵ_2, peaking at 105 ms over left, central channels ($F_{2,291} = 25.527$, $p_{cFWE} < .001$) and at 113 ms over frontal channels ($F_{2,291} = 5.047$, $p_{pFWE} < .001$). Closer inspection of the first effect revealed that the difference between small and large low-level pwPEs was reduced in central channels in the ESZ group compared with the CHR-P group (left peak: 105 ms, $t_{291} = 4.655$, $p_{cFWE} = .028$; right peak: 152 ms, $t_{291} = 4.289$, $p_{cFWE} = .026$) (Figure 2B) and the ESZ group versus the HC group (peak: 105 ms, $t_{291} = 7.141$, $p_{cFWE} < .001$) (Figure 2A). The second effect again suggested a reduced difference between small and large low-level pwPEs (Figure S12). However, this effect was observed over frontal channels in the ESZ group versus the HC group (peak: 113 ms, $t_{291} = 5.673$, $p_{\mathrm{pFWE}} < .001$) (Figure 1C) exclusively in the frequency paradigm (Figure S7). The results remained significant when parental socioeconomic status measured with the Hollingshead Four-Factor Index of Socioeconomic Status (37) was included as an additional covariate (Figure S10). The timing of these effects coincided with the timing of the MMN (8), suggesting that MMN reductions may reflect disturbances in pwPE updating processes as hypothesized previously (11,38). To investigate this further, we computed the correlations between the 10% highest minus 10% lowest ε_2 difference waveforms and the MMN in channel Cz. Both peak amplitude (defined as the most negative amplitude between 90 and 230 ms) and peak latency were significantly correlated across ε_2 difference waveforms and the MMN ($r = 0.717$, $p < .001$ and $r = .724$, $p < .001$, respectively).

Group Differences in High-Level pwPEs

The expression of high-level pwPEs about the volatility of the environment ϵ_3 also showed a significant effect of group peaking at 125 ms over right, central channels ($F_{2,291} = 17.693$, $p_{cFWE} = .007$). Pairwise comparisons revealed stronger correlations of high-level pwPEs with EEG amplitudes in the HC group than in the ESZ group over posterior central channels (peak: 344 ms, $t_{291} = 3.782$, $p_{cFWE} = .018$) (Figure 3C). Moreover, we found that the difference between small and large pwPEs was reduced during an early time window in the ESZ group versus the CHR-P group over right central channels (peak: 129 ms, $t_{291} = 5.078$, $p_{cFWE} = .011$) (Figure 3B) and in ESZ individuals versus HCs (peak: 125 ms, $t_{291} = 5.730$, $p_{cFWE} = .006$) (Figure 3A). The results remained significant

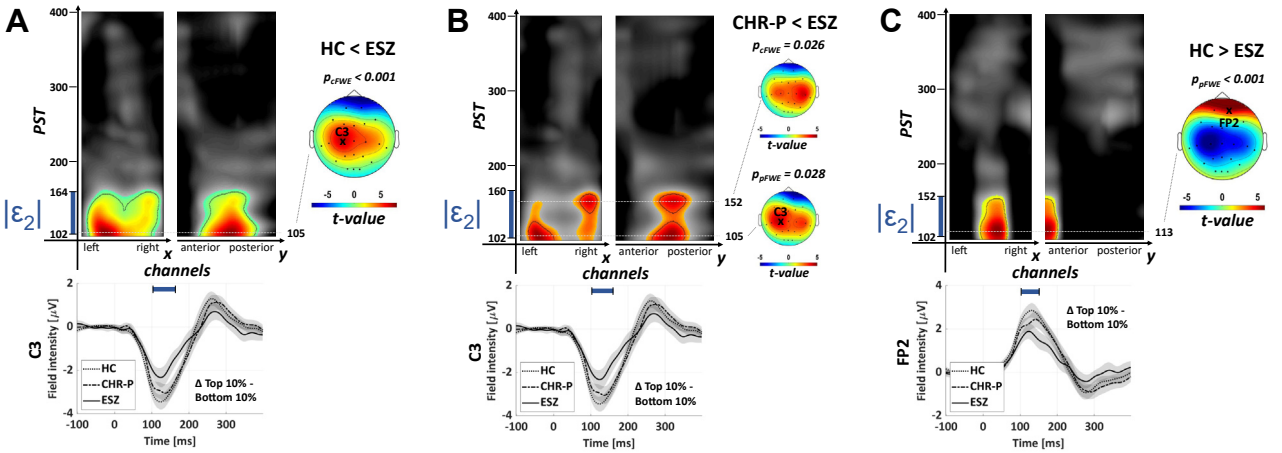

Figure 2. Low-level precision-weighted prediction errors $|\epsilon_2|$. **(A–C)** Displayed are maximum-intensity projections highlighting significant voxels of *t*-contrasts testing for pairwise group differences in the expression of low-level precision-weighted prediction errors $|\epsilon_2|$ about the tone tendency. The blue bars next to the y-axis indicate the time window of the group effect (early and latest significant voxel). *p* Values were corrected for peak-level familywise error (FWE) rates (p_{pFWE}; black dashed line) or cluster-level FWE rates (p_{cFWE}) using a cluster-defining threshold of $p < .001$ (highlighted by colored area). For illustration, difference waveforms (10% highest minus 10% lowest $|\epsilon_2|$ trials) are shown across groups for a channel close to the peak effect (highlighted in scalp plots). Please note that the event-related potential (ERP) plot is merely meant to give an intuition of the effect; the statistical tests were performed jointly on all channels using the precision-weighted prediction errors as a parametric regressor. Note that the statistical analysis window was restricted to 100 to 400 ms following each tone (standard and deviants). CHR-P, individuals at clinical high risk for psychosis; ESZ, early-illness schizophrenia (≤5 years since initial hospitalization or initiation of antipsychotic medication); HC, healthy control; PST, peristimulus time following tone presentation.

when controlling for parental socioeconomic status (Figure S11). While the early cluster again coincided with the time window of the MMN (8), the latter cluster fell into the P3a time window instead, raising the question of whether the P3a may also reflect PE-related processing. To investigate this further, we computed the correlations between the 10% highest minus 10% lowest ϵ_3 difference waveforms and the P300 in channel Pz. Both peak amplitude (defined as the most positive amplitude between 250 and 400 ms) and peak latency were significantly correlated across ϵ_3 and P300 difference waveforms ($r = 0.909$, $p < .001$ and $r = 0.715$, $p < .001$, respectively).

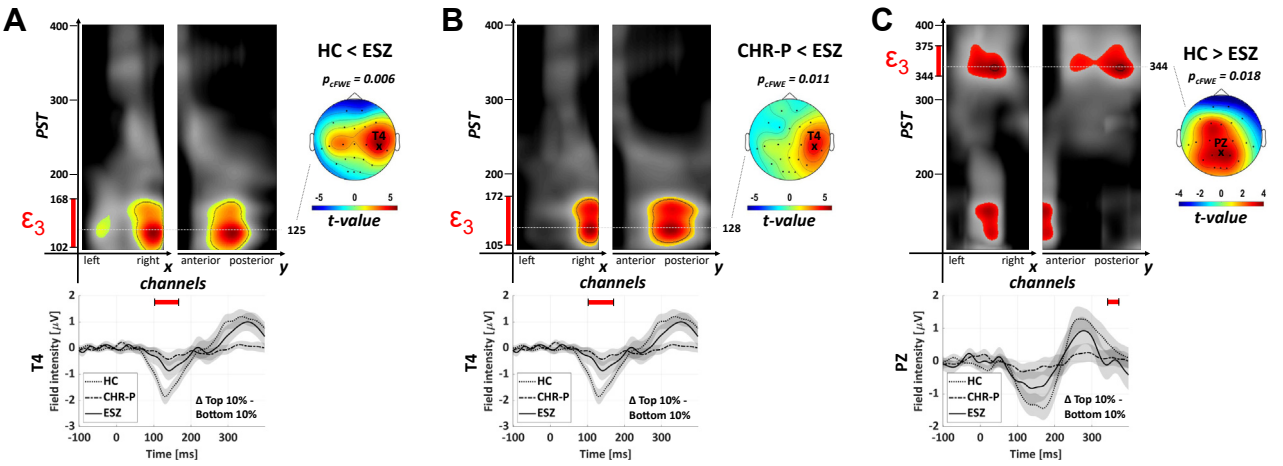

Figure 3. High-level precision-weighted prediction errors ϵ_3. **(A–C)** Displayed are maximum-intensity projections highlighting significant voxels of *t*-contrasts testing for pairwise group differences in the expression of high-level prediction errors ϵ_3 about environmental volatility. The red bars next to the y-axis indicate the time window of the group effect (early and latest significant voxel). *p* Values were corrected for peak-level familywise error (FWE) rates (p_{pFWE}; black dashedline) or cluster-level FWE rates (p_{cFWE}) using a cluster-defining threshold of $p < .001$ (highlighted by the colored area). For illustration, difference waveforms (10% highest minus 10% lowest ϵ_3 trials) are shown across groups for a channel close to the peak effect (highlighted in scalp plots). Please note that the event-related potential (ERP) plot is merely meant to give an intuition of the effect; the statistical tests were performed jointly on all channels using the precision-weighted prediction errors as a parametric regressor. Note that the statistical analysis window was restricted to 100 to 400 ms following each tone (standard and deviants). CHR-P, individuals at clinical high risk for psychosis; ESZ, early-illness schizophrenia (≤5 years since initial hospitalization or initiation of antipsychotic medication); HC, healthy control; PST, peristimulus time following tone presentation.

Group Differences Between Converters and Nonconverters

Finally, when comparing CHR-C to CHR-NC groups, we found a significant group effect on the expression of low-level pwPEs ϵ_2 peaking at 141 ms over left, central channels ($F_{1,85}$ = 13.413, p_{cFWE} = .040) (Figure S4) and an effect over frontal channels ($F_{1,85}$ = 12.643, p_{cFWE} = .043); all *p*s were small-volume corrected for the group effect on ϵ_2 between HC and ESZ groups). In the CHR-C group, the difference between small and large low-level pwPEs was reduced (central peak: 141 ms, t_{85} = 3.662, p_{cFWE} = .017) (Figure 4A) (frontal peak: 152 ms, t_{85} = 3.556, p_{cFWE} = .034) (Figure 4B); all *p*s were small-volume corrected for the group effect on ϵ_2 between HC and ESZ groups (also see Figure S13). The central effect was primarily present in the duration paradigm (Figure S8).

Symptom Correlations

We investigated correlations between the expression of low- and high-level pwPEs and positive and negative symptoms measured either with the Scale of Prodromal Symptoms (39,40) in the CHR-P group or the Positive and Negative Syndrome Scale (41) in the ESZ group. We found no significant correlations with symptom severity in the CHR-P group (all *p*s $>$ .05). In the ESZ group, there was a cluster showing a correlation between low-level pwPEs and positive symptom severity in the duration paradigm peaking at 191 ms over right posterior channels that did not survive multiple testing correction ($F_{1,33}$ = 15.321, p_{cFWE} = .171, p_{pFWE} = .247) (Figure S9).

DISCUSSION

The objective of this study was to develop and test a mechanistic model of altered information processing as a basis for MMN amplitude reductions in the CHR-P and ESZ groups. We obtained 3 major findings: First, we observed altered expression of low-level pwPEs about the tone tendency between the HC and ESZ groups and in the CHR-P group compared with the ESZ group. Second, we also identified changes in the expression of high-level pwPEs about the volatility of the environment in the ESZ group compared with both HC and CHR-P groups during an early time window (at about 100–175 ms peristimulus time), as well as during a later time window (at about 320–380 ms). Third, the expression of low-level pwPEs was significantly altered in the CHR-C group compared with the CHR-NC group, suggesting that this computational model seems to capture relevant pathophysiological mechanisms

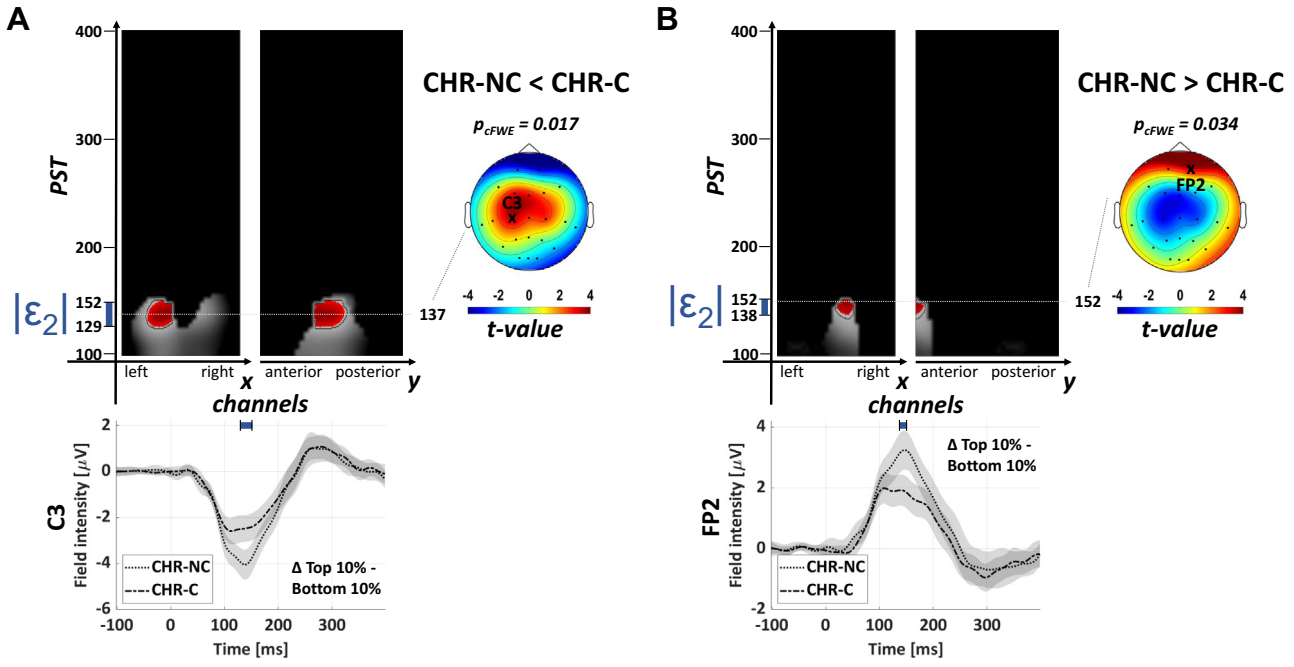

Figure 4. Low-level precision-weighted prediction errors $|\epsilon_2|$ across converters and nonconverters. **(A, B)** Displayed are maximum-intensity projections highlighting significant voxels of *t*-contrasts testing for pairwise group differences in the expression of low-level precision-weighted prediction errors $|\epsilon_2|$ about the tone tendency. The blue bars next to the y-axis indicate the time window of the group effect (early and latest significant voxel). *p* Values were corrected for peak-level familywise error (FWE) rates (p_{pFWE}; black dashed line) or cluster-level FWE rates (p_{cFWE}) using a cluster-defining threshold of $p < .001$ (highlighted by the colored area) and small volume corrected for the group effect on $|\epsilon_2|$ between the healthy control (HC) group and early-illness schizophrenia (ESZ) group (Figure S4; masked out voxels are highlighted by black color). For illustration, difference waveforms (10% highest minus 10% lowest $|\epsilon_2|$ trials) are shown across groups for a channel close to the peak effect (highlighted in scalp plots). Please note that the event-related potential (ERP) plot is merely meant to give an intuition of the effect; the statistical tests were performed jointly on all channels using the precision-weighted prediction errors as a parametric regressor. Note that the statistical analysis window was restricted to 100 to 400 ms following each tone (standard and deviants). CHR-C, individuals at clinical high risk for psychosis who later converted to a psychotic disorder; CHR-NC, individuals at clinical high risk for psychosis who did not convert; PST, peristimulus time following tone presentation.

and may constitute a useful tool for predicting transition to psychosis.

Theoretical Implications for the Predictive Coding Account of Psychosis

Our results are consistent with the predictive coding account of psychosis that postulates that disturbances in hierarchical PE processing may contribute to psychotic symptoms (20,42). More specifically, the predictive coding account suggests that overly precise bottom-up PEs and/or weakened priors may result in psychotic symptoms. Furthermore, the predictive coding account speculates that the computation of PEs and precisions may relate to AMPA receptor and NMDAR-neuromodulator interactions, respectively (20–22). Our finding of alterations in the expression of pwPEs in central channels in patients with schizophrenia (Figure 2 and Figure S12) may suggest that patients experience overly precise PEs (43) in response to familiar stimuli (standard tones) or a failure to explain away low-level PEs due to weaker high-level priors. The altered expression of hierarchical PEs in frontal channels could signal such a decrease in the precision of priors in frontal regions, as proposed in the predictive coding account of psychosis (20). Based on previous findings, we can speculate that a failure to explain away low-level pwPEs could translate into changes at higher levels, for example, expecting the environment to be more volatile as was suggested by other recent results (44–48). However, this question will need to be examined in future longitudinal studies due to the correlational nature of our findings.

Are Aberrant pwPEs Related to Alterations in Neurotransmission?

The dysconnectivity hypothesis (21,49–52) postulates that NMDAR-mediated modulation of synaptic gain is altered in schizophrenia. Consistent with this account, Weber *et al.* (14) found that ketamine administration led to reduced expression of high-level pwPEs about environmental volatility in central channels, similar to our results. However, ketamine did not affect low-level pwPEs in this study.

Several neurotransmitters interact with NMDARs to dynamically control synaptic gain and neuroplasticity. Altered expression of pwPEs in the ESZ group, as identified in our study over early auditory regions, could reflect changes in cholinergic neurotransmission. Three recent studies have implicated acetylcholine in regulating synaptic gain or—according to the predictive coding account and the dysconnectivity hypothesis—regulating sensory precision in early auditory regions (15,27,38). The first study used a Kalman filter (i.e., a 2-level HGF) to model changes in participants who were administered galantamine, which enhances cholinergic neurotransmission (38). The authors argued that galantamine may increase the precision of sensory PEs. The second study, by Schöbi *et al.* (27), modeled changes in between- and within-region connectivity including synaptic gain during a pharmacological manipulation using the muscarinic receptor antagonist scopolamine or the muscarinic receptor agonist pilocarpine in rats (27). The authors found dose-dependent changes in synaptic gain as well as changes in interregional connectivity between A1 and the secondary auditory cortex. The third study found that a single dose of the muscarinic receptor antagonist biperiden led to decreased correlations between EEG amplitudes and low-level pwPEs, but increased correlations with high-level pwPEs, which suggests a complex relationship between neurotransmitters and pwPEs (15). Moreover, changes in muscarinic receptor density among patients with schizophrenia have been reported frequently (53–56), and Scarr *et al.* (55) proposed that there may be a subgroup of patients with schizophrenia who are specifically characterized by decreased cortical muscarinic receptor expression. These results support a potential role of cholinergic neurotransmission in pwPE signaling. Beyond cholinergic processes, glutamatergic neurotransmission at AMPA receptors may be involved, but its precise role still needs to be clarified.

Clinical Implications

Interestingly, our results suggest that the expression of low-level pwPEs is blunted in CHR-C individuals compared with CHR-NC individuals. This finding highlights potential applications of this computational approach to prediction of psychosis in CHR-P individuals. Furthermore, if the neurotransmitter systems that are involved in computing pwPEs during the MMN paradigm can be identified, this approach may be useful for identifying critical time windows for preventive interventions or for predicting treatment response to pharmacological interventions that target either glutamatergic neurotransmission such as D-serine, which has shown promising results in a recent clinical trial (57), or cholinergic neurotransmission, for example involving the muscarinic (M1, M4) agonist xanomeline (58).

Limitations

Future studies should include stronger manipulations of volatility to better distinguish between different levels of hierarchical inference. Moreover, we assumed that participants acted as ideal Bayesian observers without taking subject-specific deviations from an ideal observer into account by estimating subject-specific parameters based on both sensory input and behavioral responses. This is an inherent limitation of the passive MMN oddball paradigm. In light of this limitation, our results are more challenging to interpret. Group differences could arise because different groups are better explained by different models or different model parameter values (deviations from the ideal observer). Alternatively, the model and parameter values may be appropriate, but reduced correlations with EEG data may result from altered expression of pwPEs via a loss of synchronization of pyramidal cells. While MMN amplitude reductions have been frequently replicated in schizophrenia (4), future studies should also investigate the representation of pwPEs using active oddball paradigms that require participants to detect and respond to infrequent target stimuli, such as the paradigm used in a recent study (59) that found that target P3b amplitudes were predictive of conversion to psychosis. The use of active oddball paradigms would allow the modeling of deviations from the ideal observer explicitly either by estimating subject-specific parameters based on both input and participants' behavior or by performing model comparison. Moreover, our results were obtained from a small

sample of patients and still need to be replicated in a larger study. Finally, we were unable to assess the effects of race/ethnicity due to the small sample size.

Future Directions

Future studies should determine the cortical generators of changes in the expression of hierarchical pwPEs in CHR-P individuals and early schizophrenia. Moreover, the biological implementation of these computations needs to be clarified further, for example through the use of models that include greater physiological detail to bridge the algorithmic description that our modeling approach offers and its physiological implementation in the brain (60). Dynamic causal models for electrophysiological data have been highlighted as computational assays that may allow to draw inferences about receptor densities of neuronal populations (51,61). These models have been validated in studies investigating NMDAR antibody encephalitis (28), dopaminergic action on NMDARs (29), and manipulations of cholinergic neurotransmission (27) and thus constitute a promising way forward. In addition, there is a need for more pharmacological studies with animals and humans to map the relationships between hierarchical pwPEs and different neurotransmitter systems that are targeted by antipsychotic medication.

Conclusions

In this study, we examined the computational mechanisms underlying preattentive auditory deviance processing in the CHR-P state and early schizophrenia and found evidence for aberrant expression of pwPEs at different levels of hierarchical inference. Our results suggest that the expression of low-level pwPEs is significantly altered in at-risk individuals who will later transition to psychosis, highlighting that this computational modeling approach captures relevant pathophysiological mechanisms and may prove useful for predicting transition to psychosis in CHR-P individuals.

ACKNOWLEDGMENTS AND DISCLOSURES

This work was supported by the National Institutes of Health (Grant No. R01 MH076989 [to DHM]), the Swiss National Science Foundation (Doc.Mobility, Grant No. 200054 [to DJH]), Ambizione (Grant No. PZ00P3_167952 [to AOD]), the Brain and Behavior Research Foundation (to DHM), the Krembil Foundation (to AOD), and the U.S. Department of Veterans Affairs (Veterans Affairs Senior Research Career Award No. 1IK6CX002519 [to JMF]).

A previous version of this article was published as a preprint on medRxiv: https://doi.org/10.1101/2022.12.20.22283712 and as part of DJH's Ph.D. thesis (45).

DHM is a consultant for Gilgamesh Pharmaceuticals, Neurocrine Biosciences, and Recognify Life Sciences. All other authors report no biomedical financial interests or potential conflicts of interest.

ARTICLE INFORMATION

From the Centre for Medical Image Computing, Department of Computer Science, University College London, London, United Kingdom (DJH); Krembil Centre for Neuroinformatics, Centre for Addiction and Mental Health, Toronto, Ontario, Canada (CEC, JDG, AOD); Department of Psychiatry, University of Basel, Basel, Switzerland (AS); Department of Psychiatry, University of Toronto, Toronto, Ontario, Canada (JDG, AOD); Department of Psychiatry, Yale University School of Medicine, New Haven, Connecticut (SWW, VHS); Mental Health Service, Veterans Affairs San Francisco Health Care System, San Francisco, California (JMF, DHM); Department of Psychiatry and Behavioral Sciences, University of California San Francisco, San Francisco, California (JMF, DHM); Department of Mathematics and Computer Science, University of Basel, Basel, Switzerland (VR); Institute of Medical Sciences, University of Toronto, Toronto, Ontario, Canada (AOD); and Department of Psychology, University of Toronto, Toronto, Ontario, Canada (AOD).

AOD and DHM contributed equally to this work as joint senior authors.

Address correspondence to Daniel J. Hauke, Ph.D., at d.hauke@ucl.ac.uk.

Received Jan 3, 2023; revised Jul 18, 2023; accepted Jul 20, 2023.

Supplementary material cited in this article is available online at https://doi.org/10.1016/j.bpsc.2023.07.011.

REFERENCES

1. Näätänen R, Paavilainen P, Rinne T, Alho K (2007): The mismatch negativity (MMN) in basic research of central auditory processing: A review. Clin Neurophysiol 118:2544–2590.
2. Näätänen R, Gaillard AWK, Mäntysalo S (1978): Early selective-attention effect on evoked potential reinterpreted. Acta Psychol (Amst) 42:313–329.
3. Fitzgerald K, Todd J (2020): Making sense of mismatch negativity. Front Psychiatry 11:468.
4. Erickson MA, Ruffle A, Gold JM (2016): A meta-analysis of mismatch negativity in schizophrenia: From clinical risk to disease specificity and progression. Biol Psychiatry 79:980–987.
5. Bodatsch M, Ruhrmann S, Wagner M, Müller R, Schultze-lutter F, Frommann I, *et al.* (2011): Prediction of psychosis by mismatch negativity. Biol Psychiatry 69:959–966.
6. Bodatsch M, Brockhaus-Dumke A, Klosterkötter J, Ruhrmann S (2015): Forecasting psychosis by event-related potentials-Systematic review and specific meta-analysis. Biol Psychiatry 77:951–958.
7. Hamilton HK, Boos AK, Mathalon DH (2020): Electroencephalography and event-related potential biomarkers in individuals at clinical high risk for psychosis. Biol Psychiatry 88:294–303.
8. Perez VB, Woods SW, Roach BJ, Ford JM, Mcglashan TH, Srihari VH, Mathalon DH (2014): Automatic auditory processing deficits in schizophrenia and clinical high-risk patients: Forecasting psychosis risk with mismatch negativity. Biol Psychiatry 75:459–469.
9. Haigh SM, Coffman BA, Salisbury DF (2017): Mismatch negativity in first-episode schizophrenia: A meta-analysis. Clin EEG Neurosci 48:3–10.
10. Davies C, Cipriani A, Ioannidis JPA, Radua J, Stahl D, Provenzani U, *et al.* (2018): Lack of evidence to favor specific preventive interventions in psychosis: A network meta-analysis. World Psychiatry 17:196–209.
11. Garrido MI, Kilner JM, Stephan KE, Friston KJ (2009): The mismatch negativity: A review of underlying mechanisms. Clin Neurophysiol 120:453–463.
12. Lieder F, Stephan KE, Daunizeau J, Garrido MI, Friston KJ (2013): A neurocomputational model of the mismatch negativity. PLoS Comput Biol 9:e1003288.
13. Poublan-Couzardot A, Lecaignard F, Fucci E, Davidson RJ, Mattout J, Lutz A, Abdoun O (2022): Time-resolved dynamic computational modeling of human EEG recordings reveals gradients of generative mechanisms for the MMN response. bioRxiv. https://doi.org/10.1101/2022.09.12.507526.
14. Weber LA, Diaconescu AO, Mathys C, Schmidt A, Kometer M, Vollenweider F, Stephan KE (2020): Ketamine affects prediction errors about statistical regularities: A computational single-trial analysis of the mismatch negativity. J Neurosci 40:5658–5668.
15. Weber LA, Tomiello S, Schöbi D, Wellstein KV, Mueller D, Iglesias S, Stephan KE (2022): Auditory mismatch responses are differentially sensitive to changes in muscarinic acetylcholine versus dopamine receptor function. eLife 11:e74835.
16. Friston K (2005): A theory of cortical responses. Philos Trans R Soc Lond B Biol Sci 360:815–836.
17. Wacongne C, Labyt E, Van Wassenhove V, Bekinschtein T, Naccache L, Dehaene S (2011): Evidence for a hierarchy of predictions

and prediction errors in human cortex. Proc Natl Acad Sci U S A 108:20754–20759.
18. Kiebel SJ, Daunizeau J, Friston KJ (2008): A hierarchy of time-scales and the brain. PLoS Comput Biol 4:e1000209.
19. Kiebel SJ, von Kriegstein K, Daunizeau J, Friston KJ (2009): Recognizing sequences of sequences. PLoS Comput Biol 5:e1000464.
20. Sterzer P, Adams RA, Fletcher P, Frith C, Lawrie SM, Muckli L, *et al.* (2018): The predictive coding account of psychosis. Biol Psychiatry 84:634–643.
21. Friston KJ, Brown HR, Siemerkus J, Stephan KE (2016): The dysconnection hypothesis (2016). Schizophr Res 176:83–94.
22. Javitt DC, Sweet RA (2015): Auditory dysfunction in schizophrenia: Integrating clinical and basic features. Nat Rev Neurosci 16:535–550.
23. Schmidt A, Bachmann R, Kometer M, Csomor PA, Stephan KE, Seifritz E, Vollenweider FX (2012): Mismatch negativity encoding of prediction errors predicts S-ketamine-induced cognitive impairments. Neuropsychopharmacology 37:865–875.
24. Umbricht D, Schmid L, Koller R, Vollenweider FX, Hell D, Javitt DC (2000): Ketamine-induced deficits in auditory and visual context-dependent processing in healthy volunteers: Implications for models of cognitive deficits in schizophrenia. Arch Gen Psychiatry 57:1139–1147.
25. Heekeren K, Daumann J, Neukirch A (2008): Mismatch negativity generation in the human 5HT 2A agonist and NMDA antagonist model of psychosis. Psychopharmacol (Berl) 300:77–88.
26. Frässle S, Yao Y, Schöbi D, Aponte EA, Heinzle J, Stephan KE (2018): Generative models for clinical applications in computational psychiatry. Wiley Interdiscip Rev Cogn Sci 9:e1460.
27. Schöbi D, Homberg F, Frässle S, Endepols H, Moran RJ, Friston KJ, *et al.* (2021): Model-based prediction of muscarinic receptor function from auditory mismatch negativity responses. Neuroimage 237:118096.
28. Symmonds M, Moran CH, Leite MI, Buckley C, Irani SR, Stephan KE, *et al.* (2018): Ion channels in EEG: Isolating channel dysfunction in NMDA receptor antibody encephalitis. Brain 141:1691–1702.
29. Moran RJ, Symmonds M, Stephan KE, Friston KJ, Dolan RJ (2011): An in vivo assay of synaptic function mediating human cognition. Curr Biol 21:1320–1325.
30. Mathys CD, Daunizeau J, Friston KJ, Stephan KE (2011): A Bayesian foundation for individual learning under uncertainty. Front Hum Neurosci 5:39.
31. Mathys CD, Lomakina EI, Daunizeau J, Iglesias S, Brodersen KH, Friston KJ, Stephan KE (2014): Uncertainty in perception and the hierarchical Gaussian filter. Front Hum Neurosci 8:825.
32. Fryer SL, Roach BJ, Hamilton HK, Bachman P, Belger A, Carrión RE, *et al.* (2020): Deficits in auditory predictive coding in individuals with the psychosis risk syndrome: Prediction of conversion to psychosis. J Abnorm Psychol 129:599–611.
33. Charlton CE, Lepock JR, Hauke DJ, Mizrahi R, Kiang M, Diaconescu AO (2022): Atypical prediction error learning is associated with prodromal symptoms in individuals at clinical high risk for psychosis. Schizophrenia 8:105.
34. Kiebel SJ, Friston KJ (2004): Statistical parametric mapping for event-related potentials: I. Generic considerations. Neuroimage 22:492–502.
35. Worsley KJ, Marrett S, Neelin P, Vandal AC, Friston KJ, Evans AC (1996): A unified statistical approach for determining significant signals in images of cerebral activation. Hum Brain Mapp 4:58–73.
36. Flandin G, Friston KJ (2019): Analysis of family-wise error rates in statistical parametric mapping using random field theory. Hum Brain Mapp 40:2052–2054.
37. Hollingshead AB (1975): Four Factor Index of Social Status. New Haven, CT: Yale University.
38. Moran RJ, Campo P, Symmonds M, Stephan KE, Dolan RJ, Friston KJ (2013): Free energy, precision and learning: The role of cholinergic neuromodulation. J Neurosci 33:8227–8236.
39. Miller TJ, Ph.D., Mcglashan TH, Rosen JL, Psy D, Somjee L, Markovich PJ, Stein K, Woods SW (2002): Prospective diagnosis of the initial prodrome for schizophrenia based on the structured interview for prodromal syndromes: Preliminary evidence of interrater reliability and predictive validity. Am J Psychiatry 159:863–865.
40. Miller TJ, McGlashan TH, Rosen JL, Cadenhead K, Cannon T, Ventura J, *et al.* (2003): Prodromal assessment with the structured interview for prodromal syndromes and the scale of prodromal symptoms: Predictive validity, interrater reliability, and training to reliability. Schizophr Bull 29:703–715.
41. Kay SR, Fiszbein A, Opler LA (1987): The Positive and Negative Syndrome Scale (PANSS) for schizophrenia. Schizophr Bull 13:261–276.
42. Fletcher PC, Frith CD (2009): Perceiving is believing: A Bayesian approach to explaining the positive symptoms of schizophrenia. Nat Rev Neurosci 10:48–58.
43. Kapur S (2003): Psychosis as a state of aberrant salience: A framework linking biology, phenomenology, and pharmacology in schizophrenia. Am J Psychiatry 160:13–23.
44. Hauke DJ, Wobmann M, Andreou C, Mackintosh A, de Bock R, Karvelis P, *et al.* (2023): Aberrant perception of environmental volatility during social learning in emerging psychosis. medRxiv. https://doi.org/10.1101/2023.02.02.23285371.
45. Hauke DJ (2022): Hierarchical Bayesian inference in psychosis. Switzerland: Doctoral Thesis, University of Basel. Available at: https://edoc.unibas.ch/89780/. Accessed October 5, 2023.
46. Reed EJ, Uddenberg S, Suthaharan P, Mathys CD, Taylor JR, Groman SM, Corlett PR (2020): Paranoia as a deficit in non-social belief updating. eLife 9:e56345.
47. Suthaharan P, Reed EJ, Leptourgos P, Kenney JG, Uddenberg S, Mathys CD, *et al.* (2021): Paranoia and belief updating during the COVID-19 crisis. Nat Hum Behav 5:1190–1202.
48. Cole DM, Diaconescu AO, Pfeiffer UJ, Brodersen KH, Mathys CD, Julkowski D, *et al.* (2020): Atypical processing of uncertainty in individuals at risk for psychosis. NeuroImage Clin 26:102239.
49. Friston KJ (1998): The disconnection hypothesis. Schizophr Res 30:115–125.
50. Friston KJ, Frith CD (1995): Schizophrenia: A disconnection syndrome? Clin Neurosci 3:89–97.
51. Stephan KE, Baldeweg T, Friston KJ (2006): Synaptic plasticity and dysconnection in schizophrenia. Biol Psychiatry 59:929–939.
52. Stephan KE, Friston KJ, Frith CD (2009): Dysconnection in schizophrenia: From abnormal synaptic plasticity to failures of self-monitoring. Schizophr Bull 35:509–527.
53. Scarr E, Hopper S, Vos V, Seo MS, Everall IP, Aumann TD, *et al.* (2018): Low levels of muscarinic M1 receptor–positive neurons in cortical layers III and V in Brodmann areas 9 and 17 from individuals with schizophrenia. J Psychiatry Neurosci 43:338–346.
54. Scarr E, Craig JM, Cairns MJ, Seo MS, Galati JC, Beveridge NJ, *et al.* (2013): Decreased cortical muscarinic M1 receptors in schizophrenia are associated with changes in gene promoter methylation, mRNA and gene targeting microRNA. Transl Psychiatry 3:e230.
55. Scarr E, Cowie TF, Kanellakis S, Sundram S, Pantelis C, Dean B (2009): Decreased cortical muscarinic receptors define a subgroup of subjects with schizophrenia. Mol Psychiatry 14:1017–1023.
56. Dean K, Murray RM (2005): Environmental risk factors for psychosis. Dialogues Clin Neurosci 7:69–80.
57. Kantrowitz JT, Woods SW, Petkova E, Cornblatt B, Corcoran CM, Chen H, *et al.* (2015): D-serine for the treatment of negative symptoms in individuals at clinical high risk of schizophrenia: A pilot, double-blind, placebo-controlled, randomised parallel group mechanistic proof-of-concept trial. Lancet Psychiatry 2:403–412.
58. Paul SM, Yohn SE, Popiolek M, Miller AC, Felder CC (2022): Muscarinic acetylcholine receptor agonists as novel treatments for schizophrenia. Am J Psychiatry 179:611–627.
59. Hamilton HK, Roach BJ, Bachman PM, Belger A, Carrion RE, Duncan E, *et al.* (2019): Association between P300 responses to auditory oddball stimuli and clinical outcomes in the psychosis risk syndrome. JAMA Psychiatry 76:1187–1197.
60. Marr D (1982): Vision. San Francisco: Freeman.
61. Stephan KE, Mathys C (2014): Computational approaches to psychiatry. Curr Opin Neurobiol 25:85–92.
62. Crovitz HF, Zener K (1962): A group-test for assessing hand- and eye-dominance. Am J Psychol 75:271–276.